online data

Characterization of a recombinant type II 3-deoxy-D-*arabino*-heptulosonate-7-phosphate synthase from *Helicobacter pylori*

Celia J. WEBBY*, Mark L. PATCHETT† and Emily J. PARKER*[1]

*Institute of Fundamental Sciences, Massey University, Palmerston North, New Zealand, and †Institute of Molecular Biosciences, Massey University, Palmerston North, New Zealand

DAH7P (3-Deoxy-D-*arabino*-heptulosonate 7-phosphate) synthase catalyses the condensation reaction between phosphoenolpyruvate (PEP) and D-erythrose 4-phosphate (E4P) as the first committed step in the biosynthesis of aromatic compounds in plants and micro-organisms. Previous work has identified two families of DAH7P synthases based on sequence similarity and molecular mass, with the majority of the mechanistic and structural studies being carried out on the type I paralogues from *Escherichia coli*. Whereas a number of organisms possess genes encoding both type I and type II DAH7P synthases, the pathogen *Helicobacter pylori* has only a single, type II, enzyme. Recombinant DAH7P synthase from *H. pylori* was partially solubilized by co-expression with chaperonins GroEL/GroES in *E. coli*, and purified to homogeneity. The enzyme reaction follows an ordered sequential mechanism with the following kinetic parameters: K_m (PEP), 3 μM; K_m (E4P), 6 μM; and k_{cat}, 3.3 s^{-1}. The enzyme reaction involves interaction of the *si* face of PEP with the *re* face of E4P. *H. pylori* DAH7P synthase is not inhibited by phenylalanine, tyrosine, tryptophan or chorismate. EDTA inactivates the enzyme, and activity is restored by a range of bivalent metal ions, including (in order of decreasing effectiveness) Co^{2+}, Mn^{2+}, Ca^{2+}, Mg^{2+}, Cu^{2+} and Zn^{2+}. Analysis of type II DAH7P synthase sequences reveals several highly conserved motifs, and comparison with the type I enzymes suggests that catalysis by these two enzyme types occurs on a similar active-site scaffold and that the two DAH7P synthase families may indeed be distantly related.

Key words: aromatic amino acids, 3-deoxy-D-*arabino*-heptulosonate 7-phosphate (DAHP), 3-deoxy-D-*arabino*-heptulosonate-7-phosphate synthase, *Helicobacter pylori*, shikimate.

INTRODUCTION

3-Deoxy-D-*arabino*-heptulosonate 7-phosphate (DAH7P) synthase (EC 2.5.1.54) catalyses a condensation reaction between phosphoenolpyruvate (PEP) and D-erythrose 4-phosphate (E4P) to generate DAH7P and P_i. This is the first committed step of the shikimate pathway responsible for the biosynthesis of chorismate, a precursor of aromatic compounds, including the aromatic amino acids [1]. Synthesis of aromatic amino acids is an essential metabolic function for almost all micro-organisms and plants. The shikimate pathway is absent from animals [2,3], and therefore DAH7P synthase is a potential target for new selective antimicrobial agents.

DAH7P synthases cluster into two distinct homology families based on amino acid sequence and molecular mass [4]. These two families have been denoted as type I and type II by Walker et al. [4], and more recently they have been referred to as $AroA_I$ and $AroA_{II}$ by Gosset et al. [5]. Type I DAH7P synthases are smaller than their type II counterparts, with molecular masses less than 40 kDa. Type I DAH7P synthases can be further divided on the basis of sequence similarity into two subfamilies: Iα and Iβ [6,7]. DAH7P synthases of the Iβ subfamily are more closely related to 3-deoxy D-*manno*-octulosonate 8-phosphate (KDO8P) synthases (EC 2.5.1.55) than to members of subfamily Iα [7]. KDO8P synthase catalyses an analogous reaction to DAH7P synthase involving the condensation of PEP with D-arabinose 5-phosphate (A5P), a key step in lipopolysaccharide biosynthesis in Gram-negative bacteria.

The majority of mechanistic and structural studies on DAH7P synthases have been performed on the subfamily Iα paralogues from *Escherichia coli*. These studies have shown that this type Iα DAH7P synthase catalyses an ordered sequential reaction requiring the presence of a bivalent metal [8]. The reaction has been shown to proceed via cleavage of the C–O bond of PEP and to be stereospecific with respect to the reacting faces of both substrates [9,10]. While DAH7P is found predominantly in a cyclic tautomeric form in solution, analysis of the structures is consistent with formation of an acyclic reaction intermediate [11].

Type II DAH7P synthases are larger than the type I enzymes (about 54 kDa), were identified originally in plants, and were thought to include a limited number of microbial proteins [4]. However, as more microbial genomes have been sequenced, it has been shown that type II DAH7P synthases consist of a subset of plant enzymes clustered within a more divergent set of microbial enzymes, and it has been proposed that the plant DAH7P synthases have a microbial origin [5]. In some organisms such as *Amycolatopsis mediterranei*, *Amycolatopsis methanolica*, *Xanthomonas campestris*, *Pseudomonas aeruginosa* and *Stigmatella aurantiaca*, both type I and type II DAH7P synthases have been identified [12,13]. Several of these type II enzymes have been shown to be required for the biosynthesis of specific secondary metabolites [13,14]. However, the presence of only type II DAH7P synthases in a number of micro-organisms, including *Streptomyces*, *Corynebacterium diphtheriae*, *Campylobacter jejuni*, *Agrobacterium tumefaciens*, *Novosphingobium aromaticivorans*, *Helicobacter pylori* and several mycobacteria is consistent with type II DAH7P synthases functioning in aromatic amino acid biosynthesis.

There is limited mechanistic information and no structural data available on type II DAH7P synthases. Microbial type II enzymes

Abbreviations used: A5P, D-arabinose 5-phosphate; BTP, BisTris-propane; DAH7P, 3-deoxy-D-*arabino*-heptulosonate 7-phosphate; DTT, dithiothreitol; E4P, D-erythrose 4-phosphate; G6P, D-glucose 6-phosphate; G3P, DL-glyceraldehyde 3-phosphate; IPTG, isopropyl β-D-thiogalactopyranoside; KDO8P, 3-deoxy-D-*manno*-octulosonate 8-phosphate; MMCO, molecular-mass cut-off; ORF, open reading frame; PEP, phosphoenolpyruvate; R5P, D-ribose 5-phosphate; TIM, triose phosphate isomerase.

[1] To whom correspondence should be sent, at the following address: Institute of Fundamental Sciences, Massey University, Private Bag 11-222, Palmerston North, New Zealand (email E.J.Parker@massey.ac.nz).

from *Streptomyces* and *Neurospora crassa* were characterized prior to the availability of sequence information and classification [4,15–17]. Recently Gosset et al. [5] partially purified and characterized the type II DAH7P synthase from *Xanthomonas campestris*. A more complete understanding of both the functional and structural similarities and differences between type I and type II DAH7P synthases will provide information on their evolutionary relationship and may lead to the development of type-specific chemotherapeutic agents.

H. pylori strain J99 is a pathogenic Gram-negative bacterium that colonizes the gastric and upper-intestinal epithelium of humans. This organism has been established as the major aetiological agent of active chronic gastritis, is associated with peptic ulcers and has been linked to the development of gastric cancer [18]. The single DAH7P synthase encoded by the genome of this pathogen belongs to the type II family [19]. We report here the expression, *in vivo* solubilization, purification and characterization of the DAH7P synthase from *H. pylori*. *In vivo* solubilization was achieved by co-expression of *H. pylori* type II DAH7P synthase and *E. coli* chaperonins in *E. coli*. This is the first microbial type II DAH7P synthase to be characterized where genomic information supports its role in primary metabolism.

EXPERIMENTAL

Bacterial strains, plasmids, media and growth conditions

DNA corresponding to the ORF (open reading frame) of *H. pylori* strain J99 DAH7P synthase (GenBank® accession number Q9ZMU5) was amplified from genomic DNA using Pfu Turbo DNA polymerase (Stratagene). The primers used were 5′-GATTATACATATGTCAAACACAACCTGGTCGC (forward) incorporating an NdeI restriction site and 5′-TGGGATCCATTAAGTGCGTTGTTTTTTAAGC (reverse) incorporating a BamHI restriction site. The 1.3 kbp PCR product was digested sequentially with NdeI and BamHI, gel-purified, and ligated using T4 DNA ligase (Roche) into plasmid pET-32a(+) (Novagen) previously digested with the same endonucleases. The ligation mixture was used to transform competent *E. coli* XL1-Blue (Stratagene). Plasmid miniprep DNA from transformants was used as the template in PCR reactions to identify plasmids containing the DAH7P synthase ORF. The sequence of the insert DNA in the recombinant pET-*Hpy*DAH7PS plasmids was identical with the *H. pylori* DAH7P synthase ORF. pET-*Hpy*DAH7PS was used to transform, by electroporation, *E. coli* BL21(DE3) already containing the pGroESL plasmid (generously provided by Dr George Lorimer, E. I. Dupont De Nemours and Company, Wilmington, DE, U.S.A.) [20]. Electroporation was performed using a Bio-Rad Gene Pulser (200 Ω, 25 μF, 2.5 kV, 0.2 cm gap). For expression of recombinant *H. pylori* strain J99 DAH7P synthase, BL21(DE3)/pGroESL/pET-*Hpy*DAH7PS was grown in Luria–Bertani broth containing ampicillin (100 $\mu g \cdot ml^{-1}$) and chloramphenicol (25 $\mu g \cdot ml^{-1}$) at 37 °C in baffled flasks (1 litre of medium/4 litre flask) with shaking (150 rev./min) until mid-exponential phase [attenuance (D_{600}) ≈ 0.4–0.6]. The growth temperature was then lowered to 25 °C and IPTG (isopropyl β-D-thiogalactopyranoside; Applichem, Darmstadt, Germany) added to a final concentration of 1 mM. The cells were harvested (6400 ***g*** for 20 min) 6 h post-induction and stored at − 70 °C.

Enzyme purification

Purification was carried out at 4 °C in 1 day in view of the apparent instability of the enzyme. Frozen cell pellets were resuspended in lysis buffer (4 °C) consisting of BTP (BisTris-propane) buffer (10 mM, adjusted to pH 7.5 with 10 M HCl), dithiothreitol (DTT; 2 mM), Thesit™ [dodecylpoly(ethylene glycol ether)$_n$ ($n = 9$–10); 0.005 %] and PEP (200 μM). The cells were lysed by sonication on ice for volumes less than 1 ml, and by French Press [55.2 MPa (8000 lbf/in^2)] for larger volumes. Cell debris was removed by centrifugation (26 712 ***g*** for 15 min). The supernatant fraction was diluted 5-fold with buffer A [50 mM BTP (pH 8.5)/1 mM DTT] and loaded on to a column (8 ml) of Source 15Q® (Amersham) equilibrated in buffer A at 4 °C. The unbound protein was removed with 2 column vol. of buffer A, and the bound protein was eluted with a 50 ml linear gradient between buffer A and buffer A + 0.33 M NaCl, at a flow rate of 1.5 $ml \cdot min^{-1}$. Active fractions (1 ml) were pooled, concentrated using a 20 ml Vivaspin 10000-MMCO (molecular-mass cut-off) concentrator (Vivascience AG, Hannover, Germany), diluted 5-fold with buffer B [50 mM BTP (pH 6.5)/1 mM DTT] and loaded on to a Mono® S (5/5) column (Amersham) equilibrated in buffer B at 4 °C. The unbound protein was removed with 2 column vol. of buffer B, and the bound protein was eluted with a 45 ml linear gradient between buffer B and buffer B + 1 M NaCl at a flow rate of 0.7 $ml \cdot min^{-1}$. Active fractions (1 ml) were pooled and concentrated using a 2 ml Vivaspin 10000-MMCO concentrator. The enzyme preparation could be further purified using size-exclusion chromatography (see below), and, in subsequent purifications, a Source 15S® column was substituted for the Mono S® column with similar results. Protein concentrations were determined by the method of Bradford [21], using BSA as a standard. It should be noted that a substantial amount of protein was lost throughout the purification, as fractions pooled were selected for purity rather than for total enzyme recovery.

Enzyme assays

The assay system for DAH7P synthase was a modified form of the assay used by Schoner and Herrmann [22]. The consumption of PEP was monitored at 232 nm ($\varepsilon = 2.8 \times 10^3\ M^{-1} \cdot cm^{-1}$ at 30 °C) using a Varian Cary 1 UV–visible spectrophotometer. Measurements were made using 1-cm-path-length quartz cuvettes. Standard reaction mixtures contained PEP (98 μM) (Sigma), E4P (270 μM) (Sigma), and $MnSO_4$ (94 μM) (Sigma) in BTP buffer (50 mM, pH 7.5). PEP and E4P solutions were made up in buffer and then treated with Chelex (Bio-Rad). The $MnSO_4$ solution was made up with BTP buffer that had been pre-treated with Chelex. The reaction was initiated by the addition of enzyme to give a final volume of 1 ml. Initial rates of reaction were determined by a least-squares fit of the initial-rate data. A unit of enzyme activity was defined as the loss of 1 μmol of PEP/min at 30 °C.

Michaelis–Menten kinetics

For the determination of the kinetic mechanism, PEP (9.9–32.5 μM) and E4P (20–200 μM) concentrations were varied at different fixed concentrations of the other substrate with $MnSO_4$ (94 μM) in BTP (50 mM, pH 7.5) buffer. Reactions were initiated by the addition of purified *H. pylori* DAH7P synthase (0.005 mg).

DAH7P for product-inhibition studies was obtained by purification of a large-scale reaction between E4P and PEP catalysed by *E. coli* DAH7P synthase as previously described [23]. DAH7P generated in this way was purified by anion-exchange chromatography (Source 15Q®), using ammonium bicarbonate (0–500 mM, pH 8) as eluent. Fractions containing DAH7P were pooled and freeze-dried. The assay mixtures used to determine DAH7P inhibition with respect to PEP contained E4P (120 μM), PEP (10, 20, 50 or 100 μM), $MnSO_4$ (100 μM) and

DAH7P (0, 1 or 2 mM). Mixtures used to determine inhibition with respect to E4P contained PEP (250 μM), E4P (10, 20, 50 and 100 μM), $MnSO_4$ (100 μM) and DAH7P (0, 1 or 2 mM). Reactions were initiated by the addition of purified *H. pylori* DAH7P synthase (0.006 mg) and duplicate assays were performed for all reaction conditions.

Metal activation

H. pylori DAH7P synthase apoenzyme was prepared by incubation with EDTA (0.5 mM, pH 8.0) for 30 min at 4 °C prior to the assay. The assay mixture contained PEP (196 μM), E4P (135 μM), and 100 μM metal salt (except $CdSO_4$, 300 μM) in BTP buffer (50 mM, pH 7.5, with EDTA (10 μM)). All solutions (except the metal salts) were pre-treated with Chelex. The reaction was initiated by the addition of apoenzyme (0.01 mg).

Effect of DTT

H. pylori DAH7P synthase (0.2 mg $\cdot$ ml^{-1}) was partially inactivated by incubation at 4 °C for 24 h in BTP buffer (50 mM, pH 7.5), retaining approx. 20 % of its original activity. Re-activation with DTT was determined by preincubating the enzyme in the presence or absence of 1 mM DTT at 30 °C for 10 min prior to the initiation of the assay. Standard assay conditions were used with the addition of enzyme to the cuvette followed by initiation with E4P.

Determination of molecular mass

Size-exclusion chromatography (Superdex-200®, Amersham) was used to determine the molecular mass of *H. pylori* DAH7P synthase in solution by comparing elution volumes with those for molecular-mass standards (MW-GF-200; Sigma). BTP (10 mM, pH 7.0) supplemented with PEP (200 μM), $MnSO_4$ (100 μM) and DTT (1 mM) was used to elute both DAH7P synthase and the standards at a flow rate of 0.4 ml $\cdot$ min^{-1}.

Substrate specificity

Assays to determine activity with G3P (DL-glyceraldehyde 3-phosphate) and G6P (D-glucose 6-phosphate) contained 250 μM PEP and 6 mM G3P (Sigma) or 1 mM G6P (Sigma). To determine the kinetics for PEP, the reaction mixture contained either 4–505 μM PEP and 10 mM A5P (Sigma) or 8 mM R5P (D-ribose 5-phosphate; Research Organics Inc., Cleveland, OH, U.S.A.) or 5.5 mM 2-deoxyR5P (Sigma). To determine the kinetics for the phosphate sugar, the reaction mixture contained 300 μM PEP and 1–15 mM A5P, 202 μM PEP and 1–15 mM R5P, or 253 μM PEP and 0.5–30 mM 2-deoxyR5P. To confirm that the C_8 sugar was formed from PEP and R5P, a large-scale reaction was carried out. PEP and R5P were dissolved in water (2.5 ml) and $MnSO_4$ was added (to give a final concentration of 100 μM). The pH of the solution was adjusted to 7.1 with 10 M NaOH. The total volume was made up to 3 ml, *H. pylori* DAH7P synthase was added (0.13 mg) and the reaction was monitored at 250 nm. After the loss of PEP had ceased, the mixture was filtered to remove enzyme (10 000-MMCO ultrafiltration device) and the product was purified by anion-exchange chromatograpy (Source 15Q®, eluted with a 175 ml linear gradient of 0–500 mM ammonium bicarbonate). Fractions containing product were pooled and freeze-dried. The white solid was redissolved in ^2H_2O and analysed by ^{1}H-NMR (Bruker Avance 400).

Facial selectivity of the *H. pylori* DAH7P synthase-catalysed reaction

(*Z*)-3-FluoroPEP (> 95 % stereochemically pure) was synthesized as described in [24]. The reaction mixture initially contained (*Z*)-3-fluoroPEP (1 mM), E4P (100 μM) and $MnSO_4$ (100 μM), in buffer (50 mM BTP, pH 7.5). *H. pylori* DAH7P synthase (0.05 mg) was added, and the disappearance of 3-fluoroPEP was monitored at 232 nm ($\varepsilon = 1.25 \times 10^3$ M$^{-1} \cdot$ cm^{-1}). As the reaction rate decreased due to depletion of substrates, more E4P and 3-fluoroPEP were added (to a final total concentration of 4 mM for 3-fluoroPEP and 1.5 mM for E4P). When the reaction had ceased, the reaction mixture was treated with Chelex, filtered (10 000-MMCO filter), dissolved in ^2H_2O and analysed by ^{19}F-NMR (Bruker Avance 400). ^{19}F chemical-shifts were referenced to monofluorotrichloromethane.

Inhibition studies

Solutions of L-phenylalanine (Sigma), L-tyrosine (Sigma) and L-tryptophan (Sigma) in water alone or in combination were added to standard assay reaction mixtures (PEP (75 μM), E4P (61 μM) and $MnSO_4$ (100 μM) in BTP buffer (50 mM, pH 7.5) to give a final total aromatic amino acid concentration of 250 μM. The reaction was initiated by the addition of *H. pylori* DAH7P synthase (0.02 mg). A freshly prepared 10 mM solution of chorismic acid (10 mM) was added to an assay solution (300 μM PEP, 100 μM E4P and 100 μM $MnSO_4$) to give final concentrations of 200 μM or 400 μM.

SDS/PAGE analysis

SDS/PAGE was performed with a 4%-(w/v)-total-acrylamide stacking gel and a 12%-(w/v)-total-acrylamide separating gel, using a Mini Protean III cell (Bio-Rad). All samples were prepared without boiling, except for whole-cell samples, which were boiled for 1 min. Low-range SDS/PAGE molecular-mass standards (Bio-Rad) were used. Gels were stained for protein using Coomassie Brilliant Blue R-250 (Park Scientific Limited, Northampton, U.K.).

RESULTS

Cloning of DAH7P synthase and co-expression with *E. coli* chaperonins

SDS/PAGE analysis of BL21(DE3)/pET-*Hpy*DAH7PS whole cells showed an overexpressed protein of the predicted subunit molecular mass for *H. pylori* DAH7P synthase (50 873 Da). After cell lysis and centrifugation this protein was evident only in the pellet fraction [see supplementary Figure S1 (http://www.biochemj.org/bj/390/bj3900223add.htm), lane 6], and no DAH7P synthase activity was detected in the supernatant. Standard strategies to improve the solubility of recombinant heterologous protein in *E. coli* such as altering growth temperature or changing the lysis buffer were investigated without success. Co-expression of *H. pylori* DAH7P synthase with *E. coli* chaperonins, however, yielded soluble protein.

Analysis of BL21(DE3)/pGroESL/pET-*Hpy*DAH7PS after growth, lysis and centrifugation, showed that $\approx$65 % of *H. pylori* DAH7P synthase was present in the supernatant fraction [see supplementary Figure S1 (http://www.biochemj.org/bj/390/bj3900223add.htm), lane 3] and that this fraction was active. The addition of salt (KCl), detergents (Thesit and n-octyl β-D-glucopyranoside), EDTA or metal ($MnSO_4$) to the lysis buffer did not additionally enhance the solubility of the recombinant DAH7P synthase.

Purification of DAH7P synthase

A two-step purification procedure based on the theoretical pI (7.5) of *H. pylori* DAH7P synthase was developed [see supplementary

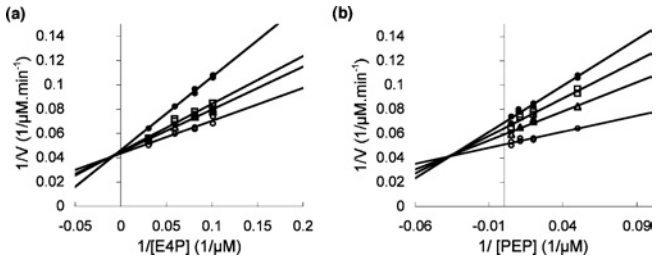

Figure 1 Determination of the kinetic mechanism of *H. pylori* DAH7P synthase

(**a**) Double-reciprocal plots of initial velocities of DAH7P synthase as a function of E4P concentration at different PEP concentrations [32.5 μM (○), 16.8 μM (△), 12.3 μM (□) and 9.9 μM (●)]. (**b**) Double-reciprocal plots of initial velocities of DAH7P synthase as a function of PEP concentration at different E4P concentrations [200 μM (○), 100 μM (△), 50 μM (□) and 20 μM (●)].

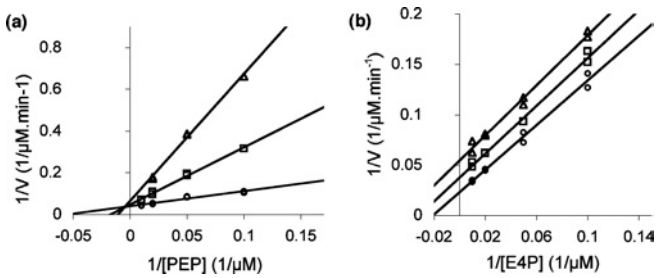

Figure 2 Product inhibition of *H. pylori* DAH7P synthase with DAH7P

Double-reciprocal plots of initial velocities are given as a function of (**a**) PEP when the DAH7P concentration was zero (○), 1 mM (□) or 2 mM (△) or (**b**) E4P when the DAH7P concentration was zero (○), 1 mM (□) or 2 mM (△).

Table 1 Effect of bivalent metals and EDTA on DAH7P synthase activity

Bivalent-metal ion	Activity (%)
Co^{2+}	100
Mn^{2+}	76
Ca^{2+}	58
Mg^{2+}	33
Cu^{2+}	12
Zn^{2+}	5
Cd^{2+}	2
Ni^{2+}	1
EDTA-treated	≈0

Table S1 and Figure S2 (http://www.biochemj.org/bj/390/bj3900223add.htm)]. The GroEL protein was substantially separated from *H. pylori* DAH7P synthase by anion-exchange chromatography. Fractionation by cation-exchange chromatography yielded a further increase in purity, with a single band of ≈51 kDa seen on SDS/PAGE analysis.

In the presence of DTT (1 mM) the enzyme maintains activity for at least 24 h at 4 °C; without DTT approx. 80 % of the enzyme activity was lost. Incubation of this partially inactivated enzyme with DTT fully restored enzymic activity. *H. pylori* DAH7PS appears to be indefinitely stable at − 70 °C when stored in the presence of 1 mM DTT at concentrations greater than 5 mg/ml.

Molecular-mass determination of *H. pylori* DAH7P synthase

The molecular mass of *H. pylori* DAH7P synthase was estimated to be 100 kDa by size-exclusion chromatography, indicating that the *H. pylori* DAH7P synthase is present as a dimer in solution.

Kinetic properties of *H. pylori* DAH7P synthase

For determination of kinetic mechanism, double-reciprocal plots were generated from initial velocity measurements determined as a function of the concentration of one substrate at various fixed concentrations of the other substrate. These plots show intersecting lines consistent with a sequential rather than ping-pong kinetic mechanism (Figure 1). K_m values for PEP and E4P were 3 ± 1 and 6 ± 1 μM respectively and the k_{cat} value for the reaction was 3.3 ± 0.3 s^{-1}. DAH7P was found to be a competitive inhibitor with respect to PEP ($K_i \approx 270$ μM) and uncompetitive with respect to E4P ($K_i \approx 1.5$ mM) (Figure 2). These results are consistent with a mechanism in which DAH7P binds to the same enzyme form as PEP, indicating that an ordered sequential mechanism is operating for *H. pylori* DAH7P synthase where PEP binds first to the enzyme and DAH7P is the last product released.

Metal activation of DAH7P synthase

The apoenzyme exhibited no detectable activity. Enzyme activity could be restored by the inclusion of a variety of bivalent metals in the activity assay (Table 1), but Zn^{2+}, Cd^{2+} and Ni^{2+} were relatively poor cofactors.

Facial selectivity of the DAH7P synthase catalysed reaction

While it is evident from the *arabino* configuration of the product that the *re* face of the aldehyde is attacked by PEP in the reaction, the use of a PEP analogue that distinguishes between the two *geminal* protons is required to determine the face of the enol phosphate that is involved. (*Z*)-3-FluoroPEP acts as an alternative substrate to PEP for *H. pylori* DAH7P synthase (V_{max} approx. 20 % of that with PEP). This compound was used to determine the stereochemical course of the enzymic reaction, by allowing (*Z*)-3-fluoroPEP to react with E4P and determine the position of fluorine in the product. The proton-coupled ^{19}F-NMR spectrum of the product 3-fluoroDAH7P showed a single resonance at − 206.6 p.p.m. that was split with coupling constants of 49.1 and 30.1 Hz (Figure 3a). This spectrum is identical with that obtained when the phenylalanine-sensitive *E. coli* type I DAH7P synthase is used to catalyse the reaction [23]. The coupling constant values indicate that the fluorine occupies an axial position and that (3*S*)-3-fluoroDAH7P is generated in the enzymic reaction (Figure 3b). It is therefore reasonable to conclude that the *H. pylori* DAH7P-synthase-catalysed reaction proceeds via interaction of the *si* face of PEP [equivalent to the *re* face of (*Z*)-3-fluoroPEP] and the *re* face of E4P.

Substrate specificity

A number of monosaccharide phosphates were tested as alternative substrates to E4P. The C_3 G3P and the C_6 G6P were not substrates for the *H. pylori* DAH7P synthase. A variety of C_5 sugar phosphates in which the C-2 hydroxy group was either absent (2-deoxyR5P) or in either possible configuration (A5P and R5P) were able to act as substrates (Table 2). A large-scale reaction of PEP with R5P catalysed by *H. pylori* DAH7P synthase was allowed to take place. The ^{1}H-NMR spectrum of the product isolated after purification was identical with the reported data for 3-deoxy-D-*altro*-octulosonate 8-phosphate [25].

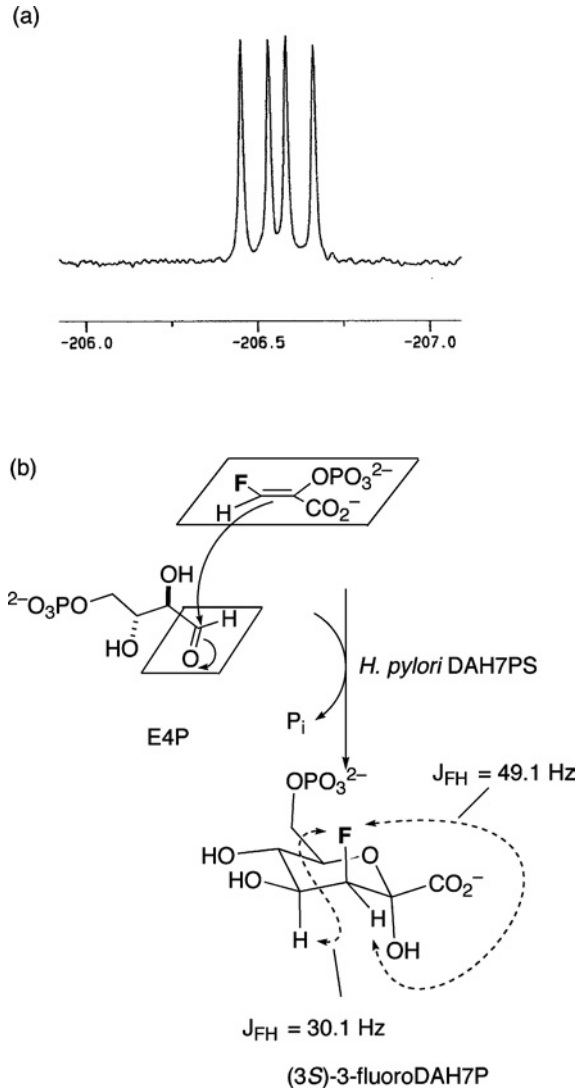

Figure 3 Stereochemical course of the *H. pylori*-catalysed DAH7P synthase reaction

(**a**) ^{19}F NMR spectrum (376 MHz) of product obtained by reaction of (*Z*)-3-fluoroPEP with E4P catalysed by *H. pylori* DAH7P synthase. (**b**) Generation of (3*S*)-3-fluoroDAH7P. The axial position of the fluorine is confirmed by the large diaxial vicinial ^{19}F–^{1}H coupling constant of 30.1 Hz.

Table 2 Substrate specifity of *H. pylori* DAH7P synthase

Kinetic constants when various monosaccharide phosphates were used as substrates for *H. pylori* DAH7P synthase are given. No enzyme activity was detected with G3P or G6P as substrates. Abbreviation: mono, monosaccharide phosphate.

Substrate	K_m (mono) (μM)	K_m(PEP) (μM)	k_{cat} (s^{-1})	k_{cat}/K_m (mono)
E4P	6 ± 1	3 ± 1	3.3 ± 0.3	0.55
R5P	1700 ± 400	1.4 ± 1	3.5 ± 0.2	0.002
2-deoxyR5P	2300 ± 500	5.2 ± 0.7	0.95 ± 0.06	0.0004
A5P	4800 ± 360	8 ± 1	0.3 ± 0.01	0.00006

Feedback inhibition studies

L-Tryptophan, L-tyrosine and L-phenylalanine, either alone or in combination, had no detectable effect on the activity of *H. pylori* DAH7P synthase. Similarly, chorismate had no effect on enzyme activity.

DISCUSSION

As with the type Iα DAH7P synthases, the type II enzymes are found in both bacterial and eukaryotic phylogenetic domains, and the function of several microbial type II DAH7P synthases in secondary metabolism can be predicted by analysis of genomic context. Some of these predictions have been experimentally verified by gene-disruption studies and by metabolite analyses. For example, the type II enzyme in *A. mediterranei* and the two type II enzymes identified in *Streptomyces collinus* have been proposed to catalyse the formation of 4-amino-3,4-dideoxy-D-*arabino*-heptulosonate 7-phosphate (aminoDAH7P) as part of the synthesis of 3-amino-5-hydoxybenzoic acid (a precursor of rifamycin, ansatrienin and naphthomycin) in the aminoshikimate pathway [14,26,27]. In organisms such as *H. pylori*, where the singular DAH7P synthase belongs to the type II family, the genomic context is not helpful in assigning a metabolic role. However, the presence of ORFs encoding other shikimate-pathway enzymes and the absence any other reported solution for the biosynthesis of DAH7P implies a role for these type II enzymes in primary metabolism.

Co-expression of *H. pylori* DAH7P synthase

The expression of *H. pylori* DAH7P synthase in *E. coli* gave rise to insoluble protein. Among the numerous strategies that have been developed to overcome the problem of inclusion-body formation in *E. coli*, co-expression of molecular chaperones is becoming increasingly popular [28]. On the basis of the observation of Houry et al. [29] that *E. coli* DAH7P synthases are substrates for *E. coli* chaperonins, we co-expressed GroEL/GroES and the *H. pylori* type II DAH7P synthase, obtaining soluble (and active) recombinant protein. The *E. coli* type I DAH7P synthases belong to the aldolase superfamily [11], a member of the TIM (triosephosphate isomerase) β/α-barrel fold. While an evolutionary relationship between type I and type II enzymes has not been established, some automated servers [30] predict that the *H. pylori* DAH7P synthase is structurally related to the type I enzymes. Structural studies are required to resolve the classification of the type II DAH7P synthases and to inform research into their evolutionary origin.

Purification and stability of *H. pylori* DAH7P synthase

The instability of the enzyme necessitated the development of a rapid, two-step, purification. Enzyme instability was also observed by Gosset et al. [5] during the purification of type II DAH7P synthase from *X. campestris*. DTT was found to protect *H. pylori* DAH7P synthase from loss of activity at 4 °C, and DTT also restored activity to partially inactivated protein. DTT activation has been reported for a number of type II DAH7P synthases. Plant DAH7P synthases have been shown to be hysteretically activated by DTT [31], and recently it has been reported that an *Arabidopsis* isoenzyme requires reduced thioredoxin for activity [32]. DTT enhanced the maintenance of activity of the microbial type II DAH7P synthases from *S. aureofaciens* and *S. coelicolor* [4,33]. By contrast, the activity of the unstable partially purified DAH7P synthase from *X. campestris* was not enhanced by DTT [5]. Whereas the activity of type I DAH7P synthases appears to be dependent on conserved cysteine residues, no particular requirement for reducing reagents has been reported [34].

Characterization of *H. pylori* DAH7P synthase

The K_m values for *H. pylori* DAH7P synthase are broadly in line with the kinetic constants reported for other type II DAH7P synthases (Table 3).

Table 3 Comparison of properties of microbial type II DAH7P synthases

The characterization of the *H. pylori* and *X. campestris* DAH7P synthases was performed on recombinant protein, whereas the other enzymes listed were purified from native sources. As it is now known that some of these organisms possess more than one type II paralogue, it is possible that the original characterizations were performed on mixtures of isoenzymes.

Organism	K_m(PEP) (μM)	K_m(E4P) (μM)	Feedback inhibition	Activation by bivalent metal (decreasing order of effect)	Reference
H. pylori	3	6	No	Co^{2+}, Mn^{2+}, Ca^{2+}, Mg^{2+}, $Cu^{2+}$and Zn^{2+}	This study
X. campestris	130	230	Tryptophan/chorismate	Co^{2+}, Zn^{2+}, Mn^{2+}, Ni^{2+}, Mg^{2+}, Ca^{2+}, Cu^{2+} and Fe^{2+}	[5]
S. coelicolor	92	195	Tryptophan	Not reported	[4]
*S. caespitosus**	430	220	Tryptophan	Co^{2+}, Zn^{2+} or Mn^{2+} restored activity to EDTA treated enzyme. Ni^{2+}, Fe^{2+} and Ca^{2+} inhibited activity.	[35,36]
*S. rimosus**	6.7	2.6	Tryptophan	Not reported	[17]
*S. aureofaciens**	300	160	Tryptophan (partial)	Partial inactivation with EDTA	[33,37]
N. crassa	12	2.7	Tryptophan	EDTA-sensitive	[16]

* No amino acid sequence information is available for these enzymes, however the DAH7P synthases from these species are highly likely to be type II enzymes, as they all have subunit molecular masses of about 50 kDa.

H. pylori DAH7P synthase activity is dependent on the presence of a bivalent-metal ion. Whereas metal dependency is also a feature of the type I enzymes, there appears to be considerable variation in the ability of different metals to activate the enzyme [8,38–40]. These studies also indicate that the *H. pylori* type II DAH7P synthase catalyses an ordered sequential reaction with defined stereochemistry as seen for type I DAH7P synthases [10,41]. The results are consistent with a reaction mechanism where E4P binds to the PEP–DAH7P synthase complex and phosphate is released from the enzyme before DAH7P. PEP presents its *si* face for reaction with E4P. The ability of the *H. pylori* type II DAH7P synthase to accept C_5, but not C_3 or C_6 sugar phosphates, as alternatives to the natural substrate E4P, albeit relatively poorly, parallels observations made with the type I phenylalanine-sensitive enzyme [25].

As for *H. pylori* DAH7P synthase, which is a dimer, other type I and type II DAH7P synthases are reported to be either dimeric or tetrameric [4,11,12,38–40]. *H. pylori* DAH7P synthase activity was unaffected by the addition of aromatic amino acids or chorismate, whereas other microbial type II enzymes [4,5,12,17,33,35] are at least partially inhibited by L-tryptophan. The *X. campestris* enzyme is also inhibited by chorismate [5]. Plant type II DAH7P synthases also appear to be insensitive to feedback inhibition by aromatic amino acids, and in some cases aromatic amino acids have even been reported to enhance enzyme activity [2,32]. The activities of type Iα DAH7P synthases are typically inhibited by one of the aromatic amino acids [42,43]. For the type Iβ DAH7P synthases, both inhibition and lack of inhibition have been reported [39,40]. Allosteric inhibition of the type I enzymes has been shown to be related to the presence of N-terminal domains and extended loops additional to the core TIM $(\beta/\alpha)_8$ barrel structure [43–45].

Analysis of type II DAH7P sequences

A ClustalX [46] alignment of type II DAH7P synthases [see the supplementary material (http://www.biochemj.org/bj/390/bj3900223add.htm) for species names and gene identifiers] shows that these enzymes have several sequence motifs that are absolutely conserved across phylogenetically diverse species (e.g. bacteria, fungi, *Toxoplasma gondii* and plants). A subgroup of sequences with an approx. 45-amino-acid deletion between residues 185 and 229 (*H. pylori* numbering) can be identified [5]. This deletion appears to be a characteristic of DAH7P synthases involved in secondary-metabolite biosynthesis where either chorismate or shikimate is a precursor. The region corresponding to *H. pylori* residues 185–229 shows relatively poor amino-acid-

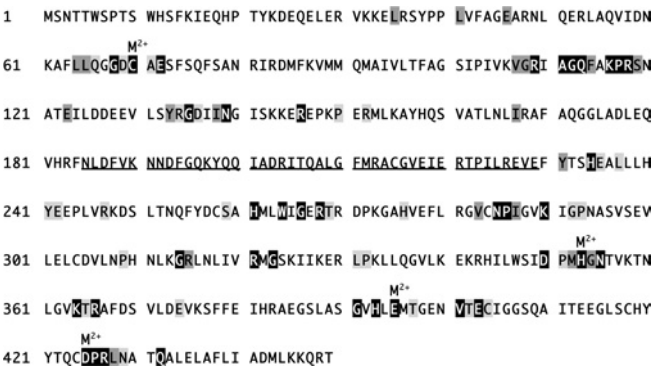

Figure 4 Pattern of conserved residues within the type II DAH7P synthases

Conserved residues are shown in relation to the *H. pylori* J99 DAH7P synthase sequence (GI:15611192). Conserved residues were identified from a multiple alignment (ClustalX) of 103 type II enzyme sequences. Invariant residues are highlighted in black, positions where unlimited conservative subsitutions are observed are highlighted in dark grey, and positions with fewer than five non-conservative variations are highlighted in light grey. The large deletion (Δ185–229, *H. pylori* numbering) found in some type II DAH7P synthases associated with secondary metabolite production is underlined. Sequences included in ClustalX alignment are listed with their gene identifiers (where available) in the supplementary material (http://www.biochemj.org/bj/390/bj3900223add.htm).

sequence conservation in full-length type II DAH7P synthases, and it has been suggested that this region dictates allosteric specificity towards chorismate and tryptophan [5] (Figure 4).

The identification of conserved residues within the type II family also provides insight into the relationship between the two enzyme families. Whereas the overall sequence identity between type I and type II DAH7P synthases is low [6], comparison of this alignment with sequence and structural information available for type I DAH7P synthases shows that key residues implicated in substrate binding and catalysis are conserved between the two enzyme families [11,47,48]. Metal-binding ligands for the type II DAH7P synthases can be proposed (Figure 4), and residues associated with both PEP and E4P binding are found in the same order and relative spacing in the primary sequence in both enzyme types. This analysis, together with the observations that the type II enzyme from *H. pylori* catalyses a metal-dependent ordered sequential reaction following the same stereochemical course as shown for type I DAH7P synthases, suggests that catalysis by these two enzyme types occurs on a similar active-site scaffold and that the two DAH7P synthase families may indeed be distantly related. Many of the questions concerning the mechanism of

the type II DAH7P synthases and the evolutionary relationship between the two DAH7P synthase families will be addressed by future functional and structural studies. The purification and characterization of the recombinant enzyme presented here is a crucial step towards this goal. Crystallization trials with the *H. pylori* DAH7P synthase are currently underway.

We thank Michael Lane (Institute of Molecular Biosciences, Massey University) for the *H. pylori* strain J99 genomic DNA. C.J.W. is a recipient of a Massey University Vice Chancellor's Doctoral Scholarship. This work was funded by the Royal Society of New Zealand Marsden Fund (MAU008).

REFERENCES

1 Bentley, R. (1990) The shikimate pathway – a metabolic tree with many branches. Crit. Rev. Biochem. Mol. Biol. **25**, 307–384
2 Herrmann, K. M. and Weaver, L. M. (1999) The shikimate pathway. Annu. Rev. Plant Physiol. Plant Mol. Biol **50**, 473–503
3 Roberts, C. W., Roberts, F., Lyons, R. E., Kirisits, M. J., Mui, E. J., Finnerty, J., Johnson, J. J., Ferguson, D. J. P., Coggins, J. R., Krell, T. et al. (2002) The shikimate pathway and its branches in apicomplexan parasites. J. Infect. Dis. **185**, S25–S36
4 Walker, G. E., Dunbar, B., Hunter, I. S., Nimmo, H. G. and Coggins, J. R. (1996) Evidence for a novel class of microbial 3-deoxy-D-*arabino*-heptulosonate-7-phosphate synthase in *Streptomyces coelicolor* A3(2), *Streptomyces rimosus* and *Neurospora crassa*. Microbiology **142**, 1973–1982
5 Gosset, G., Bonner, C. A. and Jensen, R. A. (2001) Microbial origin of plant-type 2-keto-3-deoxy-D-*arabino*-heptulosonate 7-phosphate synthases, exemplified by the chorismate- and tryptophan-regulated enzyme from *Xanthomonas campestris*. J. Bacteriol. **183**, 4061–4070
6 Jensen, R. A., Xie, G., Calhoun, D. H. and Bonner, C. A. (2002) The correct phylogenetic relationship of KdsA (3-deoxy-D-*manno*-octulosonate 8-phosphate synthase) with one of two independently evolved classes of AroA (3-deoxy-D-*arabino*-heptulosonate 7-phosphate synthase). J. Mol. Evol. **54**, 416–423
7 Subramaniam, P. S., Xie, G., Xia, T. and Jensen, R. A. (1998) Substrate ambiguity of 3-deoxy-D-*manno*-octulosonate 8-phosphate synthase from *Neisseria gonorrhoeae* in the context of its membership in a protein family containing a subset of 3-deoxy-D-*arabino*-heptulosonate 7-phosphate synthases. J. Bacteriol. **180**, 119–127
8 Stephens, C. M. and Bauerle, R. (1991) Analysis of the metal requirement of 3-deoxy-D-*arabino*-heptulosonate-7-phosphate synthase from *Escherichia coli*. J. Biol. Chem. **266**, 20810–20817
9 DeLeo, A. B. and Sprinson, D. B. (1968) Mechanism of 3-deoxy-D-*arabino*-heptulosonate-7-phosphate (DAHP) synthetase. Biochem. Biophys. Res. Commun. **32**, 873–877
10 Onderka, D. K. and Floss, H. G. (1969) Steric course of the chorismate synthetase reaction and the 3-deoxy-D-*arabino*-heptulosonate 7-phosphate (DAHP) synthetase reaction. J. Am. Chem. Soc. **91**, 5894–5896
11 Shumilin, I. A., Kretsinger, R. H. and Bauerle, R. H. (1999) Crystal structure of phenylalanine-regulated 3-deoxy-D-*arabino*-heptulosonate-7-phosphate synthase from *Escherichia coli*. Structure (London) **7**, 865–875
12 Kloosterman, H., Hessels, G. I., Vrijbloed, J. W., Euverink, G. J. and Dijkhuizen, L. (2003) (De)regulation of key enzyme steps in the shikimate pathway and phenylalanine-specific pathway of the actinomycete *Amycolatopsis methanolica*. Microbiology **149**, 3321–3330
13 Silakowski, B., Kunze, B. and Muller, R. (2000) *Stigmatella aurantiaca* Sg a15 carries genes encoding type I and type II 3-deoxy-D-*arabino*-heptulosonate-7-phosphate synthases: involvement of a type II synthase in aurachin biosynthesis. Arch. Microbiol. **173**, 403–411
14 Guo, J. and Frost, J. W. (2002) Kanosamine biosynthesis: a likely source of the aminoshikimate pathway's nitrogen atom. J. Am. Chem. Soc. **124**, 10642–10643
15 Nimmo, G. A. and Coggins, J. R. (1981) The purification and molecular properties of the tryptophan-sensitive 3-deoxy-D-*arabino*-heptulosonate 7-phosphate synthase from *Neurospora crassa*. Biochem. J. **197**, 427–436
16 Nimmo, G. A. and Coggins, J. R. (1981) Some kinetic properties of the tryptophan-sensitive 3-deoxy-D-*arabino*-heptulosonate 7-phosphate synthase from *Neurospora crassa*. Biochem. J. **199**, 657–665
17 Stuart, F. and Hunter, I. S. (1993) Purification and characterization of 3-deoxy-D-*arabino*-heptulosonate-7-phosphate synthase from *Streptomyces rimosus*. Biochim. Biophys. Acta **1161**, 209–215
18 Guillemin, K. J. and Salama, N. R. (2002) *Helicobacter pylori* functional genomics. Methods Microbiol. **33**, 291–315
19 Alm, R. A., Ling, L.-S. L., Moir, D. T., King, B. L., Brown, E. D., Doig, P. C., Smith, D. R., Noonan, B., Guild, B. C., DeJonge, B. L. et al. (1999) Genomic sequence comparison of two unrelated isolates of the human gastric pathogen *Helicobacter pylori*. Nature (London) **397**, 176–180
20 Goloubinoff, P., Gatenby, A. A. and Lorimer, G. H. (1989) GroE heat-shock proteins promote assembly of foreign prokaryotic ribulose bisphosphate carboxylase oligomers in *Escherichia coli*. Nature (London) **337**, 44–47
21 Bradford, M. M. (1976) A rapid and sensitive method for the quantitation of microgram quantities of protein utilizing the principle of protein–dye binding. Anal. Biochem. **72**, 248–254
22 Schoner, R. and Herrmann, K. M. (1976) 3-Deoxy-D-*arabino*-heptulosonate 7-phosphate synthase. Purification, properties, and kinetics of the tyrosine-sensitive isoenzyme from *Escherichia coli*. J. Biol. Chem. **251**, 5440–5447
23 Parker, E. J., Coggins, J. R. and Abell, C. (1997) Derailing dehydroquinate synthase by introducing a stabilizing stereoelectronic effect in a reaction intermediate. J. Org. Chem. **62**, 8582–8585
24 Stubbe, J. A. and Kenyon, G. L. (1972) Analogs of phosphoenolpyruvate. Substrate specificities of enolase and pyruvate kinase from rabbit muscle. Biochemistry **11**, 338–345
25 Sheflyan, G. Y., Howe, D. L., Wilson, T. L. and Woodard, R. W. (1998) Enzymic synthesis of 3-deoxy-D-*manno*-octulosonate 8-phosphate, 3-deoxy-D-*altro*-octulosonate 8-phosphate, 3,5-dideoxy-D-*gluco*(*manno*)-octulosonate 8-phosphate by 3-deoxy-D-*arabino*-heptulosonate 7-phosphate synthase. J. Am. Chem. Soc. **120**, 11027–11032
26 Chen, S., Von Bamberg, D., Hale, V., Breuer, M., Hardt, B., Muller, R., Floss, H. G., Reynolds, K. A. and Leistner, E. (1999) Biosynthesis of ansatrienin (mycotrienin) and naphthomycin. Identification and analysis of two separate biosynthetic gene clusters in *Streptomyces collinus* Tu 1892. Eur. J. Biochem. **261**, 98–107
27 Floss, H. G. and Yu, T.-W. (1999) Lessons from the rifamycin biosynthetic gene cluster. Curr. Opin. Chem. Biol. **3**, 592–597
28 Baneyx, F. and Palumbo, J. L. (2003) Improving heterologous protein folding via molecular chaperone and foldase co-expression. Methods Mol. Biol. **205**, 171–197
29 Houry, W. A., Frishman, D., Eckerskorn, C., Lottspeich, F. and Hartl, F. U. (1999) Identification of *in vivo* substrates of the chaperonin GroEL. Nature (London) **402**, 147–154
30 Kim, D. E., Chivian, D. and Baker, D. (2004) Protein structure prediction and analysis using the Robetta server. Nucleic Acids Res. **32**, W526–W531
31 Suzich, J. A., Dean, J. F. D. and Herrmann, K. M. (1985) 3-Deoxy-D-*arabino*-heptulosonate 7-phosphate synthase from carrot root (*Daucus carota*) is a hysteretic enzyme. Plant Physiol. **79**, 765–770
32 Entus, R., Poling, M. and Herrmann, K. M. (2002) Redox regulation of *Arabidopsis* 3-deoxy-D-*arabino*-heptulosonate 7-phosphate synthase. Plant Physiol. **129**, 1866–1871
33 Gorisch, H. and Lingens, F. (1971) 3-Deoxy-D-*arabino*-heptulosonate-7-phosphate synthase of *Streptomyces aureofaciens* Tu 24. II. Repression and inhibition by tryptophan and tryptophan analogues. Biochim. Biophys. Acta **242**, 630–636
34 Stephens, C. M. and Bauerle, R. (1992) Essential cysteines in 3-deoxy-D-*arabino*-heptulosonate-7-phosphate synthase from *Escherichia coli*. Analysis by chemical modification and site-directed mutagenesis of the phenylalanine-sensitive isozyme. J. Biol. Chem. **267**, 5762–5767
35 Yoo, J. C., Sung-Jun, K. and Jung-Jun, L. (1993) Inhibitors of 3-Deoxy-D-*arabino*-heptulosonate-7-phosphate synthetase from *Streptomyces caespitosus*. Korean J. Microbiol. **31**, 550–553
36 Yoo, J. C., Bang, H. J., Lee, E. H., Kim, S. J. and Lee, J. J. (1993) Purification and characteristics of 3-deoxy-D-*arabino*-heptulosonate-7-phosphate synthetase from *Streptomyces caespitosus*. Korean J. Microbiol. **31**, 340–345
37 Gorisch, H. and Lingens, F. (1971) 3-Deoxy-D-*arabino*-heptulosonate-7-phosphate synthase of *Streptomyces aureofaciens* Tu 24. I. Partial purification and properties. Biochim. Biophys. Acta **242**, 617–629
38 Ray, J. M. and Bauerle, R. (1991) Purification and properties of tryptophan-sensitive 3-deoxy-D-*arabino*-heptulosonate-7-phosphate synthase from *Escherichia coli*. J. Bacteriol. **173**, 1894–1901
39 Schofield, L. R., Patchett, M. L. and Parker, E. J. (2004) Expression, purification, and characterization of 3-deoxy-D-*arabino*-heptulosonate 7-phosphate synthase from *Pyrococcus furiosus*. Protein Expression Purif. **34**, 17–27
40 Wu, J., Howe, D. L. and Woodard, R. W. (2003) *Thermotoga maritima* 3-deoxy-D-*arabino*-heptulosonate 7-phosphate (DAHP) synthase: the ancestral eubacterial DAHP synthase? J. Biol. Chem. **278**, 27525–27531
41 DeLeo, A. B., Dayan, J. and Sprinson, D. B. (1973) Purification and kinetics of tyrosine-sensitive 3-deoxy-D-*arabino*-heptulosonic acid 7-phosphate synthetase from *Salmonella*. J. Biol. Chem. **248**, 2344–2353
42 Schnappauf, G., Hartmann, M., Kunzler, M. and Braus, G. H. (1998) The two 3-deoxy-D-*arabino*-heptulosonate-7-phosphate synthase isoenzymes from *Saccharomyces cerevisiae* show different kinetic modes of inhibition. Arch. Microbiol. **169**, 517–524

43 Shumilin, I. A., Zhao, C., Bauerle, R. and Kretsinger, R. H. (2002) Allosteric inhibition of 3-deoxy-D-*arabino*-heptulosonate-7-phosphate synthase alters the coordination of both substrates. J. Mol. Biol. **320**, 1147–1156
44 Hartmann, M., Schneider, T. R., Pfeil, A., Heinrich, G., Lipscomb, W. N. and Braus, G. H. (2003) Evolution of feedback-inhibited β/α barrel isoenzymes by gene duplication and a single mutation. Proc. Natl. Acad. Sci. U.S.A. **100**, 862–867
45 Shumilin, I. A., Bauerle, R., Wu, J., Woodard, R. W. and Kretsinger, R. H. (2004) Crystal structure of the reaction complex of 3-deoxy-D-*arabino*-heptulosonate-7-phosphate synthase from *Thermotoga maritima* refines the catalytic mechanism and indicates a new mechanism of allosteric regulation. J. Mol. Biol. **341**, 455–466
46 Chenna, R., Sugawara, H., Koike, T., Lopez, R., Gibson Toby, J., Higgins Desmond, G. and Thompson Julie, D. (2003) Multiple sequence alignment with the Clustal series of programs. Nucleic Acids Res. **31**, 3497–3500
47 Konig, V., Pfeil, A., Braus, G. H. and Schneider, T. R. (2004) Substrate and metal complexes of 3-deoxy-D-*arabino*-heptulosonate-7-phosphate synthase from *Saccharomyces cerevisiae* provide new insights into the catalytic mechanism. J. Mol. Biol. **337**, 675–690
48 Shumilin, I. A., Bauerle, R. and Kretsinger, R. H. (2003) The high-resolution structure of 3-deoxy-D-*arabino*-heptulosonate-7-phosphate synthase reveals a twist in the plane of bound phosphoenolpyruvate. Biochemistry **42**, 3766–3776

Received 10 February 2005/5 April 2005; accepted 26 April 2005
Published as BJ Immediate Publication 26 April 2005, doi:10.1042/BJ20050259